# Influence of Stiffness Ratio on Vortex-Induced Vibration of Cylinder with Low Aspect Ratio

**Conference Paper** · June 2018

CITATIONS
0

READS
5

**5 authors**, including:

Dênnis Gambarine
University of São Paulo
**5** PUBLICATIONS **6** CITATIONS
SEE PROFILE

Rodolfo Trentin Gonçalves
The University of Tokyo
**93** PUBLICATIONS **453** CITATIONS
SEE PROFILE

André M. Kogishi
Instituto de Pesquisas Tecnológicas
**11** PUBLICATIONS **13** CITATIONS
SEE PROFILE

André L. C. Fujarra
Federal University of Santa Catarina, Joinville, Brazil
**119** PUBLICATIONS **758** CITATIONS
SEE PROFILE

**Proceedings of the ASME 2018 37th International Conference on Ocean, Offshore and Arctic Engineering**
**OMAE2018**
**June 17-22, 2018, Madrid, Spain**

# OMAE2018-77665

# INFLUENCE OF STIFFNESS RATIO ON VORTEX-INDUCED VIBRATION OF CYLINDER WITH LOW ASPECT RATIO

**Dennis M. Gambarine**
(dgambarine@technomar.com.br)
Technomar - Engenharia Oceânica
São Paulo, SP, Brazil

**Luiz E. B. Minioli**
(luiz.minioli@ufsc.br)
Department of Mobility Engineering
Federal University of Santa Catarina
Joinville, SC, Brazil

**Rodolfo T. Gonçalves**
(goncalves@edu.k.u-tokyo.ac.jp)
Department of Ocean Technology
Policy and Environment
University of Tokyo
Kashiwa-no-ha, Kashiwa, Chiba, Japan

**André M. Kogishi**
(amkogishi@ipt.br)
IPT
Institute for Technological Research
São Paulo, SP, Brazil

**André L. C. Fujarra**
(andre.fujarra@ufsc.br)
Department of Mobility Engineering
Federal University of Santa Catarina
Joinville, SC, Brazil

## ABSTRACT

Concern over the Vortex-induced Motions (VIM) acting on offshore structures, with special focus on monocolumn and spar platforms, mooring systems have crucial importance on system movements; the system has thus been transformed into a concept study herein. A floating and rigid circular cylinder with low aspect ratio (L/D=2) was used in the experiments carried out to investigate the influence of stiffness ratio ($k_x/k_y$) on Vortex-Induced Vibration (VIV). The cylinder was mounted in an elastic base composed of four springs with differences in in-line and transverse stiffness, defining: $k_x/k_y \cong 0.3$, 0.5, 1.0, 2.0 and 3.0. The Reynolds number analysed belongs to a range between $0.2 \cdot 10^4$ and $2 \cdot 10^4$. Some good qualitative and quantitative agreements are found for in-line amplitudes, and higher $k_x/k_y$ systems demonstrate significant oscillation for low relative velocities. This variation can be seen and justified when the XY-plane trajectories were plotted. When $k_x/k_y$ is defined as 2 and 3, the traditional VIV 8-shape is illustrated for reduced velocities between 3 and 6. In contrast, the other stiffness systems do not show significant movements and, consequently, a negligible XY shape. Roll and pitch degrees of freedom have shown the motions coupled with the transverse and the in-line motions respectively. Moreover, the yaw motion did not present considerable angles. $k_x/k_y = 2$ has presented the highest lift force coefficients, without a great difference from the other aspects ratios, though. The drag force coefficient showed constant values for $k_x/k_y$ = 2 and 3, the smallest results were observed for the system $k_x/k_y$ =3.

Key Words: Floating circular cylinders, Stiffness Ratio, Vortex-induced Vibration, Low aspect ratio.

## INTRODUCTION

One of the most studied phenomena in the offshore and ocean engineering is the Vortex-induced Vibration (VIV). A bluff body submitted to constant sea currents starts to vibrate due to the pressure field around the body, which is formed by detachment of the Boundary layer, causing resonance problems in the structure. VIV occurrences in oil and gas equipment are com-

monly verified in sub-sea risers and pipelines. In both examples, these structures are circular cylinder with huge aspect ratio, in which the literature calls "infinite cylinders". VIV also directly affects the life time of equipment, due to the fatigue and the excessive motion, causing losses for the companies. Research literature focused on the vortex-induced vibration (VIV) phenomenon can be found in the literature, e.g. Bearman **[1]**, Sarpkaya **[6]** and Williamson and Govardhan **[9]**.

Vortex-induced Motion (VIM) is another phenomenon that affects offshore structures, presenting the same importance as VIV in the industry and in the literature, but VIM is commonly observed in larger structures, such as spar and monocolumn offshore platforms. Having the same hydrodynamic phenomenology as seen in VIV, but applied to circular cylinders with low aspect ratio, i.e. the ratio between Length and Diameter ($L/D < 6$); In addition to the small mass ratio ($m^* < 6$) and high periods of oscillation. Details about VIM in circular section platforms can be found in Fujarra et al. **[2]** and in Gonçalves, et al. **[4]**.

In order to understand the VIV phenomenon, in the last decades, some aspects were studied, such as: number of degrees of freedom, mass ratio, aspect ratio, stiffness ratio, geometry of the bluffy body, Reynolds number, among others. One of the first researches that analysed the effects of the ratio between the in-line and the transverse natural frequencies of the system ($f_{0x}/f_{0y}$) was Sarpkaya **[6]**. The author applied the concept to a cylinder free to oscillate in two degrees of freedom. Besides the traditional relation ($f_{0x}/f_{0y} = 1$), the author carried out the stiffness ratio equal two ($f_{0x}/f_{0y} = 2$); the maximum Reynolds number tested was about 35000. For the latter, data shows that the in-line drag coefficient can significantly increase with increasing frequency ratio. The maximum amplitudes were observed in the transverse direction and were lower for the case $f_{0x}/f_{0y} = 1$. In addition, the system $f_{0x}/f_{0y} = 2$ showed the occurrence of the high amplitudes in velocities range comparing with the first case, thus showing distinct curve shapes.

Sanchis **[8]** used the same frequency ratio concept to study cylinders with small mass ratio, placed in an elastic base allowing movements in two degrees of freedom (2-DOF), with high aspect ratio (L/D = 12) and low damping ($\zeta = 0.01$). A total of five different ratio frequencies were applied to the experiments, $f_{0x}/f_{0y}$ = 0.42, 0.87, 1.16, 1.36 and 1.44. System $f_{0x}/f_{0y} < 1$ presented little difference in the transition zone between the upper branch to lower branch compared with the $f_{0x}/f_{0y}$ = 1.16; however, in-line and frequencies results showed a similar behaviour for all the velocities tested. Yet for the cases $f_{0x}/f_{0y} > 1$, a great difference in the XY-plane trajectory was observed, followed by the appearance of a local maximum in the middle of the upper branch for the transverse amplitude curve.

Recently Srinil *et al.*[7] covered experimental and numerical VIV investigation in 2 DOF for an aspect ratio cylinder equal to 9 ($L/D = 9$) and four different frequency ratios were tested, $f_{0x}/f_{0y}$ = 1, 1.3, 1.6 and 1.85. The maximum amplitudes for the in-line and in the transversal direction were generally observed to reach the same values, 0.5D and 1.5D respectively. Different trajectories in the XY plane were compared and significant differences were found in the curve shapes, thus leading to the conclusion that the frequency ratio directly affects this parameter. For the cases $f_{0x}/f_{0y}$ = 1.6 and 1.85, the authors observed a flattening of the upper branch shape for the in-line and the transverse amplitudes.

Based on conceptual engineering, the practical application represents a low aspect ratio platform as a monocolumn or spar types, and different spring stiffness as mooring line tensions in the offshore field. In this context, the present work shows experiments with a floating circular cylinder elastically supported by springs. The aim is to understand how in-line/transverse stiffness can affect the vortex-induced vibration as well as the angular cylinder movements; these six degrees of freedom analysis are major innovation. In this regard, the authors use a stiffness ratio nomenclature, meaning the ratio between the in-line and transversal spring stiffness ($k_x/k_y$). The total of five different stiffness ratios were used, defined as $k_x/k_y \cong$ 0.3, 0.5, 1.0, 2.0 and 3. Due to the dimensions of the cylinder, the periods presented here are very short; for that reason, we used frequencies instead of period and consequently the VIV nomenclature appears in the VIM place.

Presenting the work methodology, the next chapter brings the experimental set-up of the tests performed, followed by Section 3, which discusses the results as a function of the reduced velocity. Finally, chapter 4 presents the main conclusions and perspectives of the present work.

## EXPERIMENTAL SETUP

In order to analyse the VIV response of low aspect ratio cylinder (L/D =2) submitted to different mooring conditions, experiments were carried out in a towing tank located in the Institute for Technological Research of the State of São Paulo, Brazil. The infrastructure is composed of a tank with 280 meter in length, 6.6 meter in width and 4 meters in depth. A dynamometric car equipped with a high accuracy encoder system was used for towing the models and set the velocities, respectively. Figure 1 shows a schematic illustration of the system used to support the floating cylinders and the schematic representation of the square rigid structure with corner dimension equal to 1100 mm. Four vertical aluminium bars were added to the structure to minimize the vertical distance between the spring fairlead in the cylinder to the spring fairlead fixed in the system, ensuring the distance equal to 150mm. Details of this system can be seen in the lateral view in Figure 1.

The structure was attached to the dynamo-metric car which is responsible for towing the system. The model was made of polyvinyl chloride (PVC) with a length $L = 250mm$ and an external diameter $D = 125mm$. The experiment intends to allow the

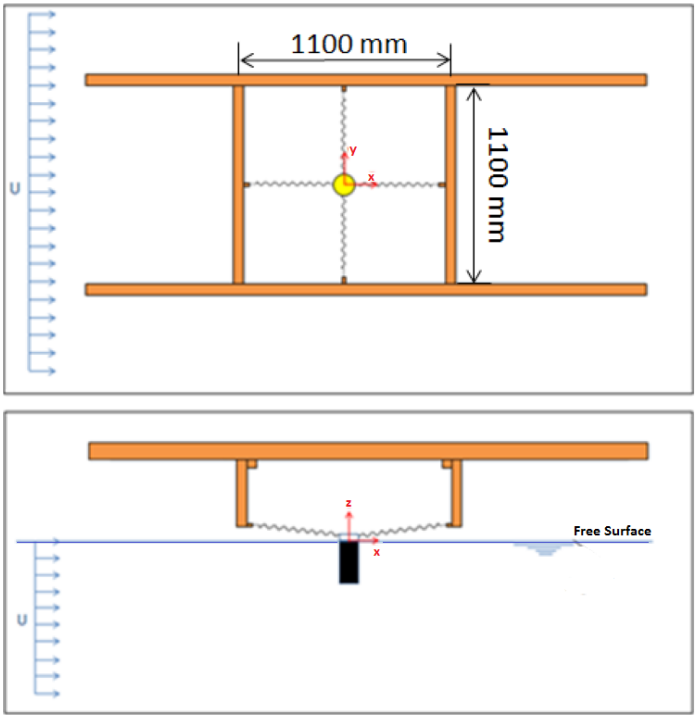


**FIGURE 1**. **Schematic top and lateral view of the system used for the experiments.**

**TABLE 1**. **Parameters of the spring stiffness and the natural frequency in still water.**

| Case | $k_x[N/m]$ | $k_y[N/m]$ | $k_x/k_y$ | $f_{ox}[Hz]$ | $f_{oy}$ $[Hz]$ |
|---|---|---|---|---|---|
| 1 | 1.10 | 3.30 | 0.33 | 0.09 | 0.12 |
| 2 | 1.60 | 3.18 | 0.52 | 0.09 | 0.12 |
| 3 | 3.10 | 3.10 | 1.00 | 0.12 | 0.12 |
| 4 | 6.50 | 3.20 | 2.03 | 0.18 | 0.11 |
| 5 | 9.60 | 3.20 | 3.00 | 0.18 | 0.12 |

**FIGURE 2**. **Experiment images of the towing tank of IPT - Institute for Technological Research of the State of São Paulo, Brazil.**

cylinder to move in six degrees of freedom (6-DOF) and to test five different stiffness spring combinations aiming to analyse the cylinder behaviour for each case. The mass ratio of the cylinder is 1 due to being a floating cylinder. The studied cases consist of two springs connected in the transverse direction, defined as $k_y$, and two more connected for in-line direction, $k_x$. The five stiffness ratio tested are defined as $k_x/k_y \cong 0.3$, 0.5, 1.0, 2.0 and 3.

Table 1 brings more details about the combinations of five different cases and the natural frequencies results for the transversal and the in-line direction in still water.

By carrying out free decay tests in still water, it was possible to estimate the damping coefficient of the system for each case. Table 2 presents details about the experiments, besides the Reynolds number and reduced velocity for each stiffness ratio. A study was conducted to define the area where the linear springs displacements work; therefore, all the results in this work contemplate the linear springs behaviour. Observe that the Reynolds numbers and reduced velocity increase when the stiffness ratio becomes larger; the reason is an excessive drift described for the model. This happens for stiffness ratios with low in-line spring stiffness where the springs start to work in the non-linear area; furthermore, some cases the downstream spring immerse into the water, consequently invalidating the results.

The motions were measured using an accurate optical (infrared) motion capture system, Qualisys. Details can be seen in Figure 3.

Throughout the study, the cylinder displacement amplitude in the X, Y and Z (in-line, transverse and heave directions) were found by the average of the 20% higher values and normalized by the cylinder diameter. The same methodology was applied to calculate the roll, pitch and yaw movements; however, these results have not been normalized by the cylinder diameter; the results are thus presented in degrees. This method judge to be perfectly acceptable for assessing the average amplitude of response for many cycles of oscillations. To find the in-line, transverse and natural system frequencies results, the Power spectrum density (PSD) was plotted and the movement frequency with higher energy characterized the value for the determined velocity. Equa-

**TABLE 2**. **Towing parameters used in the experimental texts.**

| Case | $k_x/k_y$ | $Re \cdot 10^4$ | $V_r$ |
|---|---|---|---|
| 1 | 0.33 | $0.25 \rightarrow 1.62$ | $2.0 \rightarrow 8.3$ |
| 2 | 0.52 | $0.25 \rightarrow 1.67$ | $2.0 \rightarrow 9.5$ |
| 3 | 1.00 | $0.25 \rightarrow 1.96$ | $2.0 \rightarrow 10.5$ |
| 4 | 2.03 | $0.25 \rightarrow 2.15$ | $2.0 \rightarrow 12.4$ |
| 5 | 3.00 | $0.25 \rightarrow 2.50$ | $2.0 \rightarrow 13.0$ |

**TABLE 3**. **In-line and transverse damping coefficients in still water.**

| Case | $k_x/k_y$ | $\zeta_{wx}[\%]$ | $\zeta_{wy}[\%]$ |
|---|---|---|---|
| 1 | 0.33 | $3.77 \pm 0.04$ | $2.74 \pm 0.08$ |
| 2 | 0.52 | $3.75 \pm 0.12$ | $3.45 \pm 0.10$ |
| 3 | 1.00 | $3.73 \pm 0.07$ | $2.96 \pm 0.07$ |
| 4 | 2.03 | $2.38 \pm 0.16$ | $3.07 \pm 0.20$ |
| 5 | 3.00 | $2.04 \pm 0.20$ | $3.16 \pm 0.12$ |

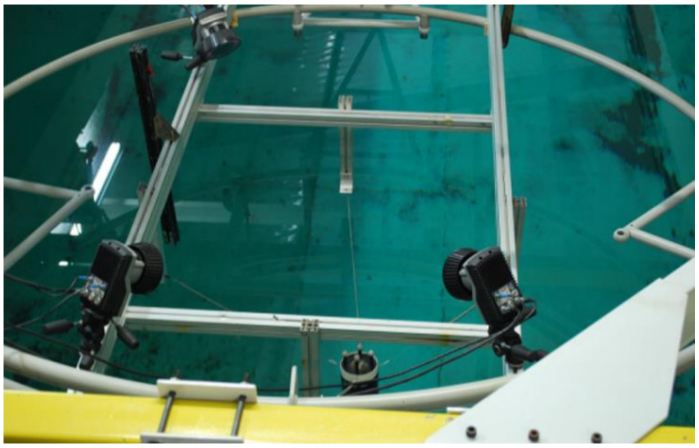

**FIGURE 3**. **Detail of the infra-red cameras used to measure the models movements.**

tion 1 presents the reduced velocity equation.

$$V_r = \frac{U}{f_{0y}D} \tag{1}$$

The pressure field around the cylinder originated by the fluid flow consequently generates lift and drag forces acting on the body. Equation 2 and 3 were used to calculate a time-dependent fluid force, where $m_s$ denotes the structural mass, $c$ the structural damping coefficient and $F_x$ and $F_y$ are the total hydrodynamic forces acting on the system in the in-line and in the transverse directions, respectively. The structural damping was disregarded in the calculations due to presenting very low values for all the systems $\zeta = 0.1\%$ .

$$m_s\ddot{x}(t) + c\dot{x}(t) + k_x x(t) = F_x(t) \tag{2}$$

$$m_s\ddot{y}(t) + c\dot{y}(t) + k_y y(t) = F_y(t) \tag{3}$$

As expected, coefficients $C_x$ and $C_y$ represent the non-dimensional drag and lift coefficients forces, respectively. The final coefficients results have used the same principle used for amplitudes, as above.

$$C_x(t) = \frac{F_x(t)}{\frac{1}{2}\rho U^2 DL} \tag{4}$$

$$C_y(t) = \frac{F_y(t)}{\frac{1}{2}\rho U^2 DL} \tag{5}$$

## EXPERIMENTAL RESULTS

This section presents the main results regarding circular cylinders free to vibrate by attaching springs. Five different stiffness combinations were used to define the ratio between the in-line and the traversal direction. This section is divided into five different results: non-dimensional amplitudes in the X, Y and Z directions (in-line, transversal and heave directions), amplitudes for roll, pitch and yaw presented in degrees, frequencies ratio analysis, lift and drag force coefficients and XY trajectory plane.

Considering the cylinder with low aspect ratio, additional effects, such as three dimensional flows, are not discussed herein, for details about how the geometry influences the fluid flow and VIV in the cylinders, check Gonalves & Fujarra **[5]** and Gambarine *et al.* **[3]**. Furthermore, free surface waves have no significant impact on the experiment results due to the small Froude number in the experiment. More information are present in Gonalves & Fujarra **[5]**.

### X, Y and Z amplitudes

The analyses regarding traversal non-dimensional amplitudes versus the reduced velocity are present in Figure 4. In

general, the behaviour of different spring systems does not directly affect this parameter. Thus, the maximum amplitudes were similar to a value $A_y/D \cong 1.4$. Note that, for the low stiffness ratio cases, $k_x/k_y \leq 1.0$, maximum velocities obtained are limited, $V_r < 10$; this occurs because the low values of stiffness applied in the in-line direction lead the model to a non-linear case, therefore preventing from seeing the lower branch transition. Sanchis **[8]** carried out similar experiments varying the stiffness ratio in the x and y directions, but the author presented different mass ratio condition in the x and y direction with experiments in two degrees of freedom. Despite the significant differences, the results presented similar behaviours for the transversal non-dimensional amplitude. For cases in which $f_{0x}/f_{0y} < 1.0$, the amplitude response was found to be similar to the case in which the frequencies are equal ($f_{0x}/f_{0y} = 1.0$). An exception was found in the transition zone between the upper and lower branches; for our case, this zone could not be presented.

Figure 5 presents the non-dimensional amplitudes for in-line direction. In contrast to the transversal amplitudes, a distinct behaviour can be observed for reduced velocities, $2.5 \leq V_r \leq 5$, in which cases with stiffness ratio equal to 2 and 3 present the highest amplitudes, $A_x/D \cong 0.12$. The maximum amplitudes occur for reduced velocities higher than 8. Case $k_x/k_y = 0.3$ presented a particular behaviour; it is possible to see the amplitude keep grows when the reduced velocity increases. Due to the experiments limitation, unfortunately, the maximum amplitude could not be recorded. On the other hand, other cases reached their maximum presenting a constant line with reduced velocities higher than eight. The smallest values can be verified when y-stiffness is twice the x-stiffness establishing the amplitudes at $A_x/D \cong 0.35$.

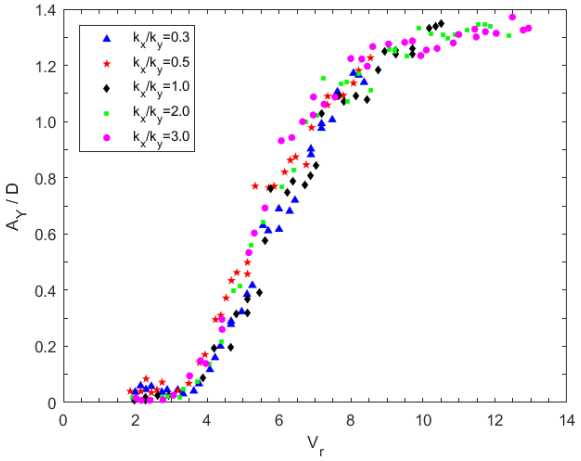


**FIGURE 4**. **Non-dimensional amplitude in the transversal direction ($A_y/D$) as a function of reduced velocity ($V_r$) for the five different stiffness ratios.**

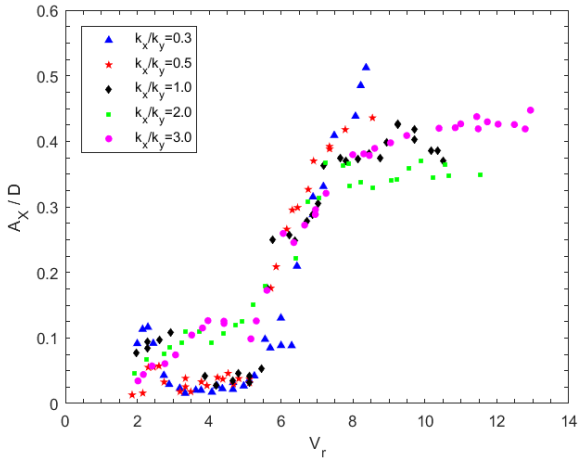


**FIGURE 5**. **Non-dimensional amplitude in the in-line direction ($A_x/D$) as a function of reduced velocity ($V_r$) for the five different stiffness ratios.**

Results concerning the "Z" direction (heave) have not shown expressive amplitudes, the maximum values achieving less than 1% of the cylinder diameter. For this reason the graph is not presented and discussed in the present paper.

## Roll, Pitch and Yaw Angular Amplitudes

Exploring the floating cylinder information, it is possible to see, for the stiffness ratio equal 3, roll angles yielding interesting and the highest values, reaching 6.5 degrees. This behaviour differs completely from the others, in which there is a gap at reduced velocity equal to 7. Moreover, system $k_x/k_y = 2$ has performed angles up to 4.0 presenting the smaller roll results as compared with the other cases. However, analysing the roll frequencies (Figure 13), we observed a similar behaviour with the frequency in the transversal direction, leading us to conclude there is coupling between the roll and transversal movements, justifying the excitation in the roll angular amplitude. Figure 6 shows the trajectories of the roll angles versus the reduced velocities obtained in the experiments.

The $k_x/k_y = 3$ system has shown the highest pitch angles through practically all the velocities, increasing as much as 2 times (for $V_r > 8$) than stiffness ratio systems up to 1, cases which in turn exhibited similar values. $k_x/k_y = 2$ presenting the second largest results regarding pitch angle, but a different behaviour occurs for reduced velocity higher than 7 when the pitch angle starts to decrease; yet this behaviour is not verified for others systems. Details can be seen in Figure 7.

Figure 8 shows the yaw angular displacement for the five stiffness conditions. Stiffness ratio higher than 1 and equal to 0.3 have presented similar results as well the largest angles compared to the others, although the velocity limit made it impossible to

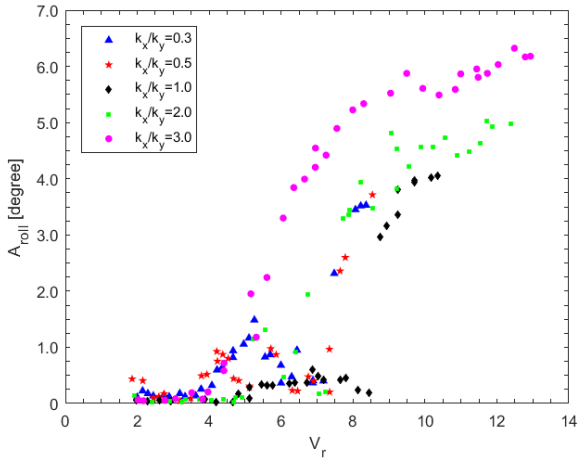


**FIGURE 6**. **Roll response amplitude ($A_{roll}/D$) as a function of reduced velocity ($V_r$) for the five different stiffness ratios.**

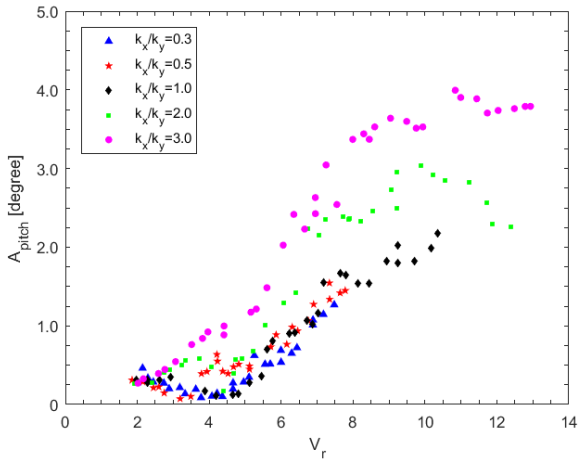


**FIGURE 7**. **Pitch response amplitude ($A_{pitch}/D$) as a function of reduced velocity ($V_r$) for the five different stiffness ratios.**

observe all the trajectory for the 0.3 case. However, the curve shape seems to grow at the same intensity as stiffness ratio higher than 1. In contrast to the outstanding angles, stiffness ratio equal 0.5 indicated maximum angles not larger than 1 degree. The experiments demonstrated that having x-stiffness twice as large as the y-stiffness yaw motion can be mitigated.

## Force Coefficients

The Experimental Set-up section described the method and equations used to generate the drag and lift coefficients. Figure 9 brings the lift coefficients values for the respective reduced velocity, and a great difference can be observed for stiffness ratios

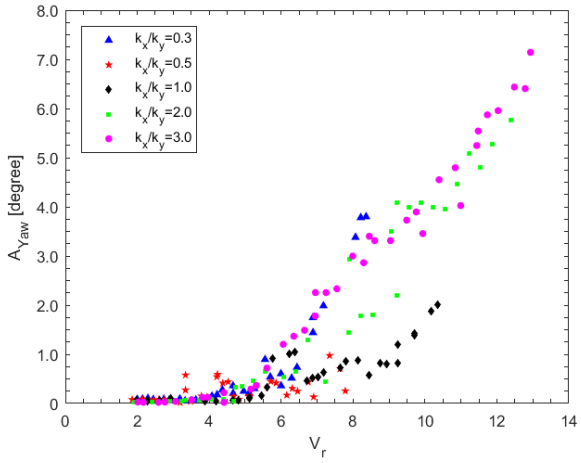


**FIGURE 8**. **Yaw response amplitude ($A_{yaw}/D$) as a function of reduced velocity ($V_r$) for the five different stiffness ratios.**

equal 0.3 and 0.5; in the initial velocities, these cases present 10 times higher coefficients as compared with others ratios. Velocities were verified to increase, however, in a range between reduced velocities 4 and 8. System $k_x/k_y = 2$ assumes the highest lift coefficients; conversely, the case with the lowest stiffness ratio presented the lowest values.

Regarding the drag coefficients, the behaviours changed significantly and case $k_x/k_y = 3$ shows the smallest results. In addition to the values, $k_x/k_y = 3$ presented a constant coefficient presenting values close to 1 for all the velocities tested. In contrast, cases with stiffness ratio up to 1 showed four times greater coefficients, but only for reduced velocities higher than 7. Those differences can be explained by the values of the in-line stiffness, i.e. when it is applying a high stiffness we expect consequently a lower force at the system.

## Frequencies

Results of the ratio between the transverse frequency and the natural frequency in still water are represented in Figure 11. A resonant motion range is observed for $2 \leq Vr \leq 3$ for all the stiffness combinations. The curves behaviour revealed certain differences; however, they obey the same trajectory. Regarding the VIV analysis, the Strouhal number ($St$) relates the vortex shedding frequency ($f_s$) with dimensional parameters of the cylinder and flow velocity. All the stiffness types presented similar Strouhal numbers, $0.10 \leq St \leq 0.11$, which allows assuming that the vortex shedding frequency is similar to the motion frequency in the transversal direction $f_s \cong f_y$, except for stiffness ratios equal to 2 and 3 at reduced velocities higher than 10.

Figure 12 presents the ratio between in-line and transverse frequency. As expected, for reduced velocities higher than six, one can be observe the couple phenomenon between the frequen-

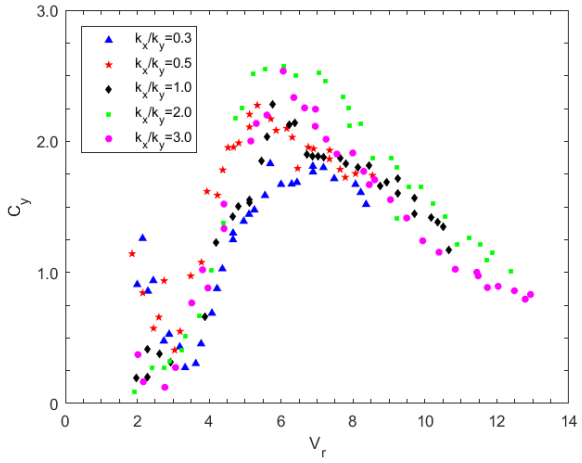


**FIGURE 9**. **Lift Coefficients ($C_y$) as a function of reduced velocity ($V_r$) for the five different stiffness ratios.**

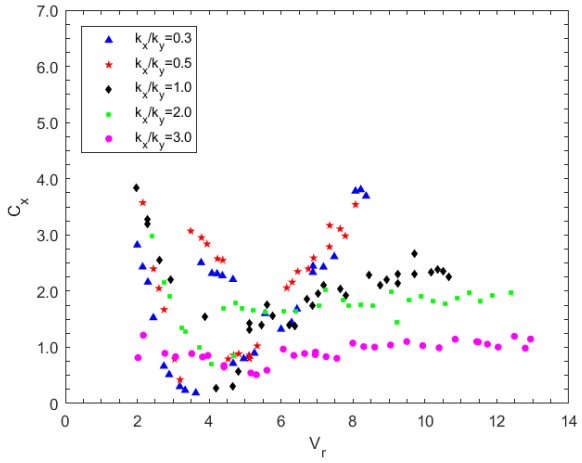


**FIGURE 10**. **Drag Coefficients ($C_y$) as a function of reduced velocity ($V_r$) for the five different stiffness ratios.**

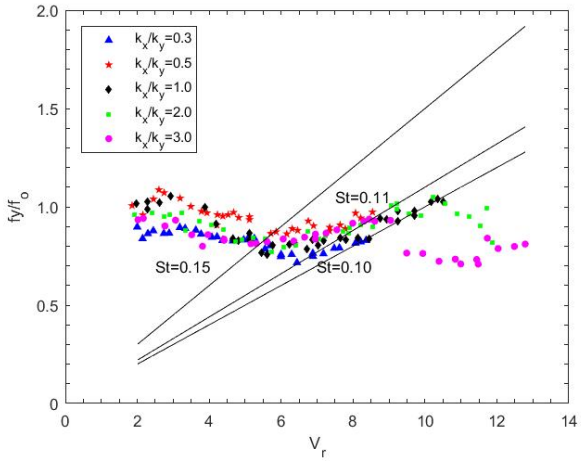


**FIGURE 11**. **Ratio between the transverse frequency and the natural frequency in still water ($f_y/f_o$) versus the reduced velocity ($V_r$) for the four cylinders.**

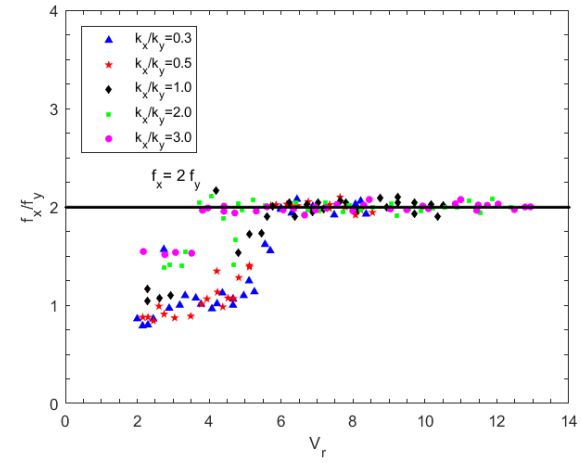


**FIGURE 12**. **Ratio between the transverse frequency and the in-line frequency ($f_x/f_y$) versus the reduced velocity ($V_r$) for the four cylinders.**

cies, i.e. when the in-line frequency is the double of the transverse frequency, $f_x \cong 2f_y$, a line is placed at this value to make the reader see the couple point more easily. That phenomenon is an example commonly seen in cylinders in VIV experiments. The differentiation at the stiffness parameters did not affect this ratio, thus there performed similarly results.

The last frequency results are shown in Figure 13 and correspond to the ratio between roll and transversal frequencies. The graph proposal is to prove the coupling between the roll and transversal motion (described in the roll angular results, Figure 6), for this purpose, the results present values close to 1.

## XY Plane

Trajectories in the XY plane (In-line/transversal plane) were studied for all the five cases, plotted together in a graph where the x-axis is represented by the reduced velocity ($V_r$), and the y-axis represents the stiffness ratio ($k_x/k_y$), separately for each case. Details can be seen in Figure 14.

Regarding the XY plane trajectories, three kinds of trajectories are observed in the results; the first case easily observed for systems $k_x/k_y \leq 1$ for the $V_r = 6$ and 8. The trajectory is similar to a crescent moon. The traditional VIV/VIM trajectory for cylindrical bodies, called 8 shape, occurs for reduced veloc-

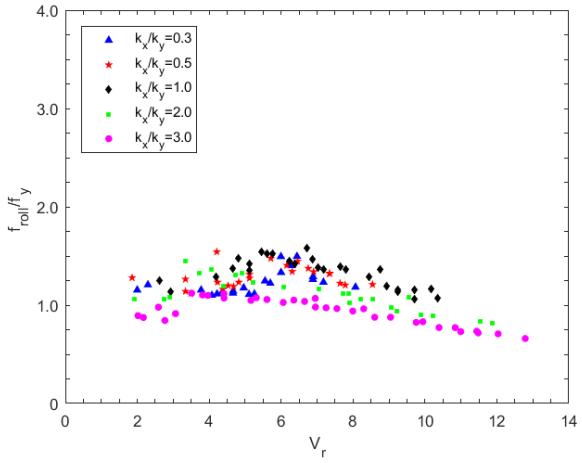


**FIGURE 13**. **Ratio between the roll frequency and the transverse frequency ($f_{roll}/f_y$) versus the reduced velocity ($V_r$) for the four cylinders.**

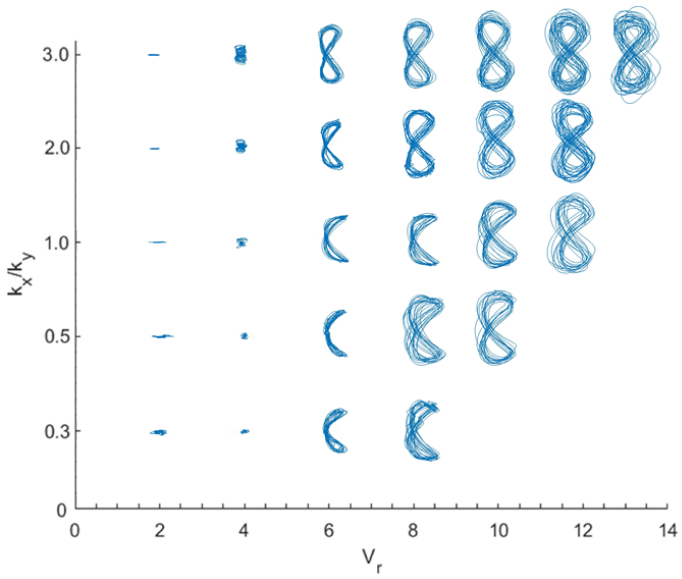


**FIGURE 14**. **XY-plane trajectory plotted on a graph; the Y-axis defines the stiffness ratio ($k_x/k_y$) and the X-axis defines the reduced velocity ($V_r$).**

ities higher than 6 for the stiffness ratio equal to 2 and 3, and is observed for high reduced velocities in cases $k_x/k_y = 0.5$ and 1. The last situation is characterized by the mix of both trajectories, can be notable for reduced velocities equal 6 and stiffness ratio 2 and 3. Sirinil *et al.* **[7]** studied the XY plane and a similar result was obtained, i.e. with less stiffness applied to the springs added to low velocities range, the "crescent moon" shape can be more easily seen.

## Conclusion

The present work was motivated by the mooring line systems used for offshore floating structures, particularly the spar and monocolumn platform types commonly used for exploration and production in deep waters. The aim was to understand the VIV effects in different stiffness ratios. A low aspect ratio cylinder was supported by springs and free to move in 6 degrees of freedom.

Analyses regarding non-dimensional transverse amplitudes showed that the stiffness ratio did not present a significant difference. Conversely, non-dimensional in-line amplitudes were 10 times superior than others in low velocities values and for $k_x/k_y = 2$ *and* 3 . In addition, $k_x/k_y = 0.3$ had a constant increase; due to experimental limitations, it was not possible to observe the maximum amplitude.

The result for lift coefficient presented a significant difference in a large range of reduced velocities, starting by the lowest lift coefficient that belongs to $k_x/k_y = 0.3$. Furthermore, the model that presented the highest coefficients was $k_x/k_y = 2$.

The in-line/traverse plane trajectory demonstrated three principal shapes. The traditional VIV trajectory, "8 shape", was developed for $k_x/k_y \geq 1$ by high velocities ($V_r \leq 10$). Systems with low stiffness ratio $k_x/k_y \leq 1$ were characterized by "crescent moon" shape. The mix between the two shapes was observed for $k_x/k_y = 2$ and 3 in the intermediating velocities.

The case in which the in-line stiffness represents twice as large as the transversal one showed to be the best arrangement to be applied, because it presented the lowest movement results in most of the cases studied. Moreover, the yaw angles yielded impressive values, not higher than 1 degree, thus holding up to hydrodynamic moments acting on the body. In turn, when the transverse stiffness is higher than the in-line condition, the movements increase as compared with other stiffness ratios at the same velocities; as well the forces applied to the springs demonstrated to be higher. The roll movements have shown angles up to 6 degrees, justified by being coupled with the transverse direction.

## NOMENCLATURE

$\zeta_s$ Structural damping

$\zeta_W$ Damping coefficient in still water

$\zeta_w x$ Damping coefficient in the in-line direction measured in still water

$\zeta_w y$ Damping coefficient in the transversal direction measured in still water

$A_x/D$ Characteristic non-dimensional motion amplitude in the in-line direction

$A_y/D$ Characteristic non-dimensional motion amplitude in the transversal direction

$A_{roll}$ Characteristic motion angle in the roll direction
$A_{pitch}$ Characteristic motion angle in the pitch direction
$A_{yaw}$ Characteristic motion angle in the yaw direction
$C_x$ Force Coefficient in the in-line direction
$C_y$ Force Coefficient in the transversal direction
$c$ Damping
$D$ Characteristic diameter
$f_0$ Natural frequency in still water, both in the in-line and in the transverse directions
$f_{0x}$ natural frequency of the system in still water in the in-line direction
$f_{0y}$ natural frequency of the system in still water in the transverse direction
$f_{roll}$ Oscillation frequency in the roll angle
$f_s$ Vortex-shedding frequency
$f_x$ Oscillation frequency in the in-line direction
$f_y$ Oscillation frequency in the transverse direction
$k$ Spring Stiffness
$k_x$ Spring Stiffness in the in-line direction
$k_y$ Spring Stiffness in the transverse direction
$m^*$ Mass ratio
$m_d$ Displaced mass
$m_s$ Structural mass
$L/D$ Aspect ratio
$Re$ Reynolds number
$U$ Flow velocity
$V_r$ Reduced velocity
$x$ In-line direction axis or displacement in the in-line direction
$y$ Transverse direction axis or displacement in the transverse direction
$\dot{x}$ In-line direction velocity
$\dot{y}$ Transverse direction velocity
$\ddot{x}$ In-line direction acceleration
$\ddot{y}$ Transverse direction acceleration

## ACKNOWLEDGMENT

The authors would like to acknowledge Petrobras and the National Petroleum and Natural Gas Agency (ANP) for the financial support. Prof. Dr. André Fujarra acknowledges the CNPq (National Council for Scientific and Technological Development, Brazil) for the financial support, grant 309591/2013-9". Dr. Rodolfo Gonçalves acknowledges the São Paulo Research Foundation (FAPESP), process number 2014/02043-1, and the University of Tokyo for the financial support.

## REFERENCES

[1] BEARMAN, P. W. Vortex Shedding from Oscillating Bluff Bodies. *Annual Review of Fluid Mechanics* Vol. 16: 195-222, 1984.

[2] FUJARRA, A. L. C., GONÇALVES, R. T., Faria F., Cueva M., Nishimoto K., Siqueira E. F. N. Mitigation of Vortex-Induced Motions of a Monocolumn Platform. *Proceedings of the 28th International Conference on Ocean, Offshore and Arctic engineering.* Honolulu, USA - OMAE2009, 2009.

[3] GAMBARINE, D. M., FIGUEIREDO, F. P., FUJARRA, A. L .C. & GONÇALVES, R. T.,Experimental study about the influence of the free end effects on vortex-induced vibration of floating cylinder with low aspect ratio. *Proceedings of the 35th International Conference on Ocean, Offshore and Arctic engineering.* OMAE2016-54632. Busan, South Korea, 2016.

[4] GONÇALVES R. T., FUJARRA A.L.C., ROSETTI G.F., NISHIMOTO K. Mitigation of Vortex-Induced Motion (VIM) on a Monocolumn Platform- Forces and Movements *Journal of Offshore Mechanics and Arctic Engineering.* 041102-16, 132. 2010.

[5] GONÇALVES, R. T., FUJARRA A.L.C. Experimental study on vortex-induced vibration of floating circular cylinders with low aspect ratio. *Proceedings of the 33st International Conference on Ocean, Offshore and Arctic engineering.* San Francisco, California, USA - OMAE2014-23383. 2014.

[6] SARPKAYA T. Hydrodynamic damping, flow-induced oscillations, and biharmonic response. *Journal of Offshore Mechanics and Arctic Engineering.* 117, 4, 232238. 1995.

[7] SRINIL N., ZANGANEH H. & DAY A. Two-degree-of-freedom VIV of circular cylinder with variable natural frequency ratio: Experimental and numerical investigations. *Journal of Ocean Engineering.* 73, 179194.2013.

[8] SANCHIS A. Two degrees of freedom vortex-induced vibrations of a rigid circular cylinder with varying natural frequencies in the x and y directions. *Proceedings of the 28th International Conference on Offshore Mechanics and Arctic Engineering.* Honolulu, USA - OMAE2009, 2009.

[9] WILLIAMSON C. H. K. & GOVARDHAN R. Vortex-induced Vibrations. *Annual Review of Fluid Mechanics.* Volume 36, pp 413-455, 2004.